

Role of the density in the crossover region of *o*-terphenyl and poly(vinyl acetate)

A. Barbieri, G. Gorini, and D. Leporini*

*Dipartimento di Fisica "Enrico Fermi," Università di Pisa, via F. Buonarroti 2, I-56127 Pisa, Italy
and INFM, Unità di Ricerca di Pisa, via F. Buonarroti 2, I-56127 Pisa, Italy*

(Received 19 December 2003; revised manuscript received 6 April 2004; published 21 June 2004)

The coupling between the reorientation of molecular probes and the density in one low-molar mass glass former [*o*-terphenyl (OTP)] and one polymer [poly(vinyl acetate) (PVAc)] is studied in the Goldstein's crossover region where the structural (α) and the secondary (β) relaxations bifurcate. The coupling is found to be strong in OTP and virtually absent in PVAc. The probes sense both the α and β relaxations, and locate their splitting accurately. It is concluded that the density affects the relaxation occurring in the crossover region of OTP but not of PVAc at subnanometer length scales. The findings are compared with recent assessments of the role of the molecular packing close and above the glass transition temperature T_g .

DOI: 10.1103/PhysRevE.69.061509

PACS number(s): 64.70.Pf, 66.30.Jt, 65.60.+a

The role of molecular packing in glass formers dynamics was early recognized by Williams [1] and Macedo and Litovitz [2]. Goldstein argued that, as the molecules in a glass-forming liquid pack more closely with decreasing temperature, the motion does not occur by free diffusion but by crossing substantial energy barriers of the energy landscape [3]. He estimated that the crossover between the two regimes takes place when the structural relaxation time is about few nanoseconds. It is the purpose of the present paper to address the role of the density in this crossover region.

Evidence that a change in the dynamics occurs comes from the bifurcation of the main α relaxation from the secondary β relaxation at a temperature T_β , above the glass transition temperature T_g , of most fragile glass formers [4–7]. Goldstein remarked that the β process may be related to the molecular packing [3], and Stillinger showed how the topography of the energy landscape accounts for the $\alpha\beta$ bifurcation [8]. Indications of a change of dynamics of the α relaxation also comes from the observed crossover between two different Vogel-Fulcher equations at a temperature $T_B \approx T_\beta$ [9–11]. The change of the relaxation mechanism above T_g is also inferred by a number of decoupling phenomena showing that the temperature dependence of the viscosity differs from the ones of other transport properties—e.g., the diffusion [5,12,13], the conductivity [14], and the rotational diffusion [15–17].

The interplay between the molecular packing and the potential energy landscape is anticipated [8,18]. However, even if the glass formers dynamics was widely investigated in the last decade as a function of both the temperature and pressure [1,19–32], there is no broad consensus if the dynamics near T_g is dominated by the density or by the available thermal energy to surmount the energy barriers or provide comparable contributions. Ferrer *et al.* [24] favor the temperature at atmospheric pressure. Dielectric [30] and Brillouin [32] relaxation studies evidenced that thermal energy and density affect on an equal footing the dynamics of supercooled low-molecular-mass van der Waals liquids at ambient pressure

and near the glass transition with notable exceptions where the density is more important [29]. For polymers T assumes a greater role [1,27,28], although volume effects are not negligible for flexible polymers [26,31]. Only for strongly hydrogen-bonded liquids [24] or polymers [25] does T appear to become dominant. Most studies compared the roles of the density and of the available thermal energy close to T_g whereas much less is known at higher temperatures. Ngai *et al.* [11] found that the thermal variations of the free volume of various glass formers, including *o*-terphenyl (OTP), reflect the crossover between two different Vogel-Fulcher regimes of the α relaxation occurring at $T_B \approx T_\beta$. Brillouin studies of OTP found that the relative contributions of temperature and density are similar [32]. Alba-Simonesco *et al.* [33] scaled the α relaxation times of some simple liquids in terms of a density- and species-dependent but T -independent effective interaction energy. Barbieri *et al.* [34] simulated a polymer melt and noted that at lower temperatures the fluctuations of the free volume and the thermal energy play similar roles whereas at high temperature the latter affects more the dynamics. Vass *et al.* [50] proposed a two-state model by defining suitable solidlike and liquidlike domains.

The accurate location of the crossover region via T_β or T_B is a delicate matter. The definition of T_β is tricky due to the usual extrapolation of the low-temperature data of the β relaxation [35]. The so-called Stickel plot offers a clear-cut definition of T_B but accurate data are needed [9]. T_B is also drawn by the intercept of two different Vogel-Fulcher equations fitting the α relaxation [11]. The electron spin resonance (ESR) spectroscopy [36] evidenced the change of the dynamics in the crossover region by monitoring the rotational dynamics of paramagnetic tracers with stiff and well-defined geometries (spin probes) being dissolved in tiny concentrations (<1 mM) [17,37]. ESR spectroscopy covers the range of correlation times 1 ps $\lesssim \tau \lesssim 0.3$ μ s. In particular, in the range 0.1 ns $\lesssim \tau \lesssim 10$ ns the ESR linewidth yields the correlation time τ of nearly spherical tracers as the area below the rotational correlation function of the spherical harmonic $Y_{2,0}$ without resorting to any rotational model [16,38,39]. Slower rates are drawn by proper reorientation models which are validated by accurate numerical simula-

*Electronic address: dino.leporini@df.unipi.it

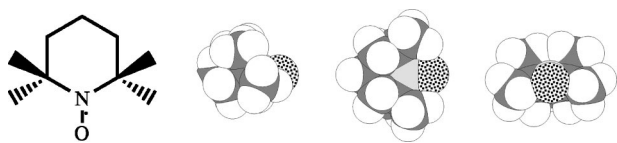


FIG. 1. Two- and three-dimensional structures of the TEMPO spin probe.

tions of the overall line shape [37]. The rotational dynamics of the spin probes takes place in the unoccupied volume, the so-called “free volume” of the host phase. Positron annihilation lifetime spectroscopy (PALS) is a nanoprobe of the free volume which is parametrized in terms of the ortho-positronium (*o*-PS) lifetime $\tau_{o\text{-PS}}$ [11,41–43]. In condensed phases *o*-PS tends to be confined in the open space of the structure where the positron is annihilated by electrons localized on the surface of the nanocavities (the penetration depth of the positron into the electron cloud is $\Delta R \approx 1.66 \text{ \AA}$ [40,41]). $\tau_{o\text{-PS}}$ increases with the size of the holes and depends on their geometry. Spherical, cubic, cuboid (rectangular parallelepiped), and elliptic holes have been considered [41,42]. To compare different spectroscopies their time and length scales must be matched. Below, it will be shown that both PALS and ESR spectroscopies probe regions as wide as a few \AA during a few nanoseconds.

We investigate the low-molecular-weight glass former OTP ($T_g = 244 \text{ K}$, fragility index $m = 81$) and the polymer poly(vinyl acetate) (PVAc, $T_g = 318 \text{ K}$, $m = 88$) for which extensive PALS [11,42] and ESR [15–17,37] data are available in the crossover region.

The ESR data refer to the rotational dynamics of two strategically chosen spin probes—namely, TEMPO and TEMPOL, the latter being a variant of TEMPO with an extra $-\text{OH}$ group in *para* position to ensure good coupling to polar groups via hydrogen bonds. TEMPO is stiff, rather compact, and the shape is almost spherical (Fig. 1). It has an average van der Waals radius $r_{\text{TEMPO}} = 3.3 \pm 0.2 \text{ \AA}$ and may be sketched as an oblate ellipsoid with semiaxes $r_{\parallel} \sim 2.7 \text{ \AA}$ and $r_{\perp} \sim 3.7 \text{ \AA}$. Since TEMPO is quite similar in size to OTP ($r_{\text{OTP}} = 3.7 \pm 0.1 \text{ \AA}$ [12]), it is expected to accommodate itself in the available free volume with negligible perturbation.

Figure 2 shows the temperature dependence of the rotational correlation time of TEMPO [15–17] and the PALS lifetime $\tau_{o\text{-PS}}$ [11] in OTP. The rotational correlation time of TEMPO τ exhibits different dynamical regimes. In region I ($T > 298 \text{ K}$) the data are well described by the Debye-Stokes-Einstein (DSE) law for a sphere, $\tau = \eta v / k_B T$, v and η being the effective volume and the shear viscosity, respectively. The apparent TEMPO radius is $r_{\text{TEMPO}}^* \approx 2.6 \text{ \AA}$ to be compared with the average van der Waals radius $r_{\text{TEMPO}} \approx 3.3 \text{ \AA}$ [17]. In region II ($280 \text{ K} < T < 298 \text{ K}$), the reorientation and viscosity decouple. The data are fit quite accurately by the fractional form of the DSE law (FDSE) $\tau \propto (\eta/T)^\xi$ with $\xi = 0.28 \pm 0.04$. Similar fractional laws were also reported for decoupling phenomena [45] involving the diffusion [12] and conductivity [14]. In region III ($T < 280 \text{ K}$) the reorientation of TEMPO is activated ($\Delta E_{\text{TEMPO}} = 19 \pm 1 \text{ kJ/mol}$ for $T > T_g$) and occurs via jumps of about 80° [15]. We stress once again that in the range

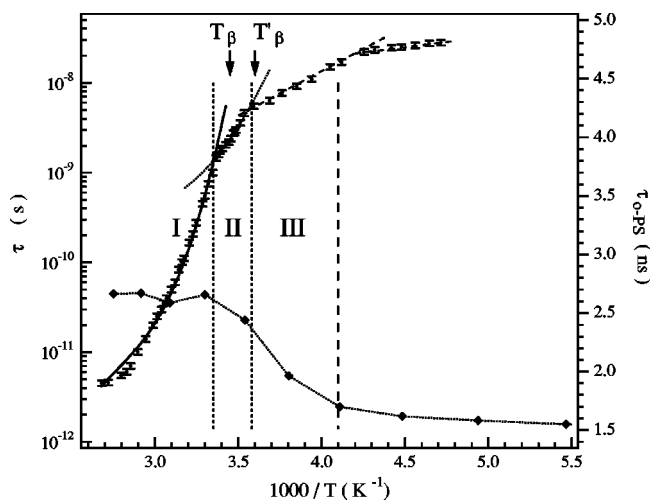


FIG. 2. Arrhenius plot of the rotational correlation time of TEMPO τ (small circles) [15–17] and the *o*-PS lifetime $\tau_{o\text{-PS}}$ (diamonds) [11] in OTP. The vertical dashed line marks T_g . The vertical dotted lines define the different dynamical regimes of the spin probe. The solid line in region I, the dotted line in region II, and the dashed lines in region III are the best fit with the DSE, the FDSE, and the Arrhenius laws, respectively. The line joining the $\tau_{o\text{-PS}}$ data is a guide for the eyes. $T_\beta = 290 \text{ K}$ and $T'_\beta = 278 \text{ K}$ refer to the splitting temperature following a quench [35,43] and a slower cooling [45] in the glassy state, respectively.

$0.1 \text{ ns} \leq \tau \leq 10 \text{ ns}$ the time τ , being defined as the area below the rotational correlation function of the spherical harmonic $Y_{2,0}$, is not derived via any specific reorientation model [16,38,39]. The crossover between the regions II and III at $T_{\text{II-III}} = 280 \text{ K}$ is remarkable. Following a quench in the glassy state the β relaxation exhibits the activation energy $\Delta E_\beta \approx 50 \text{ kJ/mol}$ [4] and merges with the α relaxation at $T_\beta = 290 \text{ K}$ [35,43]. On the other hand, for slowly cooled OTP $T'_\beta = 278 \text{ K}$ and $\Delta E'_\beta \approx 36 \text{ kJ/mol}$ are reported [44]. The sensitiveness of the β relaxation to the thermal history is known [4]. Since the ESR measurements involved slow cooling with long annealing times, it is worth noting that $T'_\beta = 278 \text{ K}$ is virtually coincident with $T_{\text{II-III}}$ and $\Delta E'_\beta / \Delta E_{\text{TEMPO}} \approx 1.9$. The above remarks lead us to the conclusion that TEMPO senses at $T_{\text{II-III}}$ the crossover between two different dynamical regimes of OTP. This is also corroborated by the observation that in region III the reorientation occurs via activated jumps [15], differently from regions I and II where the good fits of DSE and FDSE laws point to a diffusive behavior.

It is also of some interest to compare the rotational correlation time of OTP, τ_{OTP} , in the crossover region as provided by different techniques. At $T_\beta = 290 \text{ K}$ one finds $\tau_{\text{OTP}} \approx 100 \text{ ns}$ by depolarized light scattering [46,47], $\tau_{\text{OTP}} \approx \tau_\alpha \approx \tau_\beta \approx 40 \text{ ns}$ by dielectric relaxation [4], and $\tau_{\text{OTP}} \approx 80 \text{ ns}$ by NMR [12]. This must be contrasted with the rotational correlation time of different tracers dissolved in OTP. For example for the large molecules rubrene and anthracene one finds $\tau_{\text{rubrene}} \approx 500 \text{ ns}$ and $\tau_{\text{anthracene}} \approx 25 \text{ ns}$ [48]. For the much smaller TEMPO molecule we find $\tau_{\text{TEMPO}} \approx 2.2 \text{ ns}$ —i.e., about more than one order of magnitude faster than τ_{OTP} . This is ascribed to the rather symmetrical

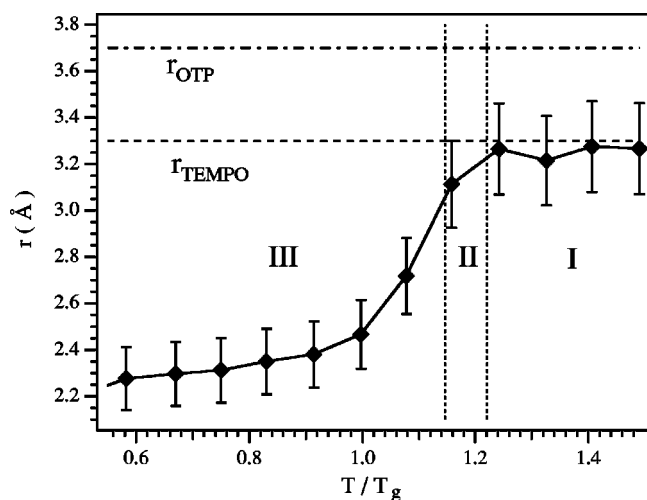


FIG. 3. Temperature dependence of the average size of the unoccupied volume r . The error bars cover the range of the values provided by different hole geometries including spheres, cuboids, and ellipsoids. The horizontal lines are the average van der Waals radii of OTP and TEMPO. The vertical dotted lines define the different dynamical regimes of the spin probe as in Fig. 2. The line joining the points is a guide for the eyes. The temperature regions are the same as Fig. 2.

shape of TEMPO which facilitates the reorientation even if the sizes of TEMPO and OTP are rather similar, $r_{\text{TEMPO}} = 3.3 \pm 0.2$ Å and $r_{\text{OTP}} = 3.7 \pm 0.1$ Å [12]. Quite interestingly, neither rubrene nor anthracene decouple from the viscosity even close to T_g [48], pointing to the conclusion that their large size limits the sensitivity to the change of the dynamics occurring at the crossover region.

Figure 2 shows that in region II, where the decoupling of the reorientation of TEMPO occurs, $\tau_{o\text{-PS}}$ drops signaling a decrease of the unoccupied volume in OTP. In this region $\tau \approx \tau_{o\text{-PS}}$ and $\tau_{o\text{-PS}}$ corresponds to unoccupied volume with size of about 3.2 Å [11]—i.e., rather comparable to $r_{\text{TEMPO}} = 3.3 \pm 0.2$ Å. This proves that PALS and ESR are probing the same length and time scales. To investigate the degree of correlation between the unoccupied volume and the rotational relaxation of TEMPO, we calculated the average size of the unoccupied volume r from $\tau_{o\text{-PS}}$ assuming that the holes are spheres, cuboids, or ellipsoids [40,41]. The aspect ratio of cuboids—i.e., square parallelepipeds—and ellipsoids was taken to be equal to the one of TEMPO. Depending on the model, $2r$ coincides, with the diameter of the sphere, the average of either the sides of the cuboid, or the axis of the ellipsoid. Figure 3 compares the temperature dependence of r and the average van der Waals radii of OTP and TEMPO, r_{OTP} and r_{TEMPO} , respectively. Due to the almost spherical shape of TEMPO, the spread of r values derived by the different models is small. In region I (refer to Fig. 2) $r \approx r_{\text{TEMPO}}$. In region II and region III $r < r_{\text{TEMPO}}$, signaling the trapping of TEMPO. r is an average quantity, so the constraints may be relaxed by favorable fluctuations of the free volume. In fact, quiescent periods followed by sudden large-angle jumps have been evidenced in region III [15]. Figure 3 proves that the change of dynamics of TEMPO in crossing region II must be ascribed to the de-

creased unoccupied volume. In view of the similar sizes of TEMPO and OTP and their good coupling, which is manifested by the change from liquidlike to solidlike reorientation of TEMPO at $T_{\text{II-III}} \approx T'_\beta$, the previous conclusion strongly suggests that OTP is primarily affected by the molecular packing in the crossover region. This parallels Ref. [11]. Brillouin studies of OTP concluded that density contributions are dominant for $T > 314$ K—i.e., more than 20 K above the crossover region—and comparable to activated contributions at lower temperatures [32]. Figure 2 shows that $T = 314$ K is well inside the liquidlike region I where neither ESR nor PALS evidences a change of dynamics. A comparison of ESR and PALS with the light scattering is difficult. Indeed, ESR and PALS are observing the same length scale, a few Å, which is rather shorter than the one of the collective dynamics investigated in Ref. [32].

The above analysis interprets the decrease of $\tau_{o\text{-PS}}$ in the crossover region of OTP and then the change of the dynamics of TEMPO in terms of higher molecular packing. A related, even if distinct, viewpoint is that the OTP molecules occupy solidlike and liquidlike states. This two-state model interpreted PALS and depolarized Raman scattering measurements in one molecular glass former [50]. In solidlike domains, thermal motion is relatively slow due to its cooperative nature involving many molecules; in liquidlike ones, the molecules tend to be separated and to move more individually and thus move more rapidly [50]. In this framework the decrease of $\tau_{o\text{-PS}}$ at lower temperatures is the signature of the smaller fraction of liquidlike molecules and the trapping of TEMPO in solidlike domains. The two-state model provides insight into the PALS results. However, it cannot be readily applied to the present study since some input parameters of the model are not reported for the PALS data on OTP under scrutiny [11].

We now turn to the PVAc case. The β relaxation of PVAc is ascribed to the motion of the polar side group which leads to, or is accompanied by, local distortions of the main chain [49]. Effective hydrogen bonding with the side group was ensured by the tracer TEMPOL. The ESR results are presented in Fig. 4. The reorientation of TEMPOL senses the α , β , and γ relaxations of PVAc and, depending on the temperature range, the rotational correlation time τ was found to be proportional ($\tau = C_i \tau_i$) to the corresponding dielectric relaxation times: $i = \alpha, T > 403$ K, $i = \beta, 403 \text{ K} > T > 273$ K, and $i = \gamma, T < 273$ K [37]. The merging temperature of PVAc is $T_\beta = 400 \pm 5$ K [7,49]. T_β compares quite well with the crossover of the TEMPOL reorientation from the α to the β dynamics occurring at 403 K.

By dielectric relaxation it is found that $\tau_\alpha \approx 40$ ns at T_β [7,51]. Gomez *et al.* modeled the merging of dielectric α and β relaxations in PVAc by using the so-called Williams-Watts ansatz [7,52]. It is shown that, on approaching T_β from below, the β relaxation departs from the low-temperature Arrhenius behavior and merges smoothly into the main relaxation at higher temperatures. The analysis yields $\tau_\beta \approx 3$ ns at T_β to be compared with $\tau_{\text{TEMPOL}} \approx 0.63$ ns at the same temperature. The results by Gomez *et al.* suggest that the crossover of the reorientation of TEMPOL from being coupled to the secondary β relaxation for $T < T_\beta$ to being coupled to the main relaxation for $T > T_\beta$ (Fig. 4) is driven

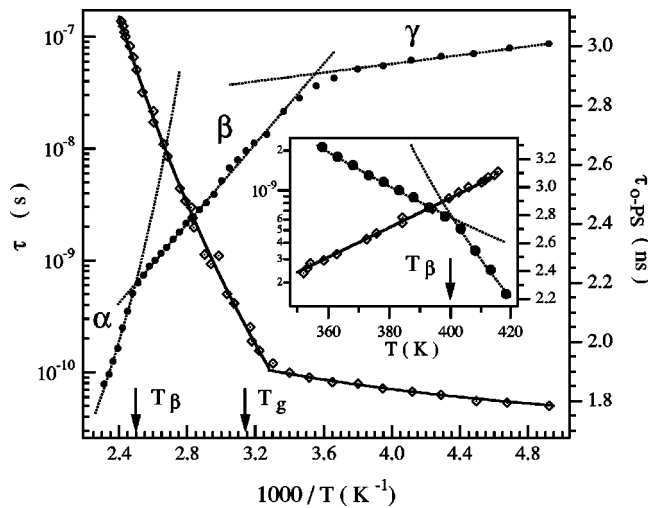


FIG. 4. Arrhenius plot of the rotational correlation time of TEMPOL τ (circles) [32] and the o-PS lifetime τ_{o-PS} (diamonds) [42] in PVAc. The dashed lines are proportional to the dielectric relaxation times τ_α ($T > 403$ K), τ_β ($403\text{K} > T > 273$ K), and τ_γ ($T < 273$ K). The solid-lines across τ_{o-PS} data are best fits with linear temperature dependences. The splitting temperature $T_\beta = 400 \pm 5$ K is marked [7,49]. The inset magnifies the temperature dependence of the PALS and ESR data in the crossover region.

by the former. This is not surprising in view of the location of TEMPOL being close to the polar side group of PVAc whose motion leads to the β relaxation [49].

In the crossover region of PVAc the rotational correlation time of TEMPOL falls in the range $0.1 \text{ ns} \lesssim \tau \lesssim 10 \text{ ns}$ where τ is not model dependent. Since τ_{o-PS} (and then the unoccupied volume) covers a dynamic range being quite similar to

the OTP case, TEMPOL has a size and shape virtually identical to TEMPO and $\tau_{o-PS}/\tau \sim 4.4$ at T_β , one concludes that PALS and ESR sense the same length and time scales also in the crossover region of PVAc. However, Fig. 4 shows that, differently from the OTP case, τ_{o-PS} exhibits no anomaly at T_β and linearly increases with temperature [42]. The corresponding smooth increase of the unoccupied volume points to the conclusion that the well-defined dynamical crossover of TEMPOL at T_β is poorly determined by the available free volume. Since TEMPOL is located closely to the the polar side group of PVAc, this conclusion may be extended to the α and β relaxations at T_β as well. The role of temperature in PVAc may be understood. For polymers T assumes a more important role [1,27,28,34]. Polar interactions in PVAc increase somewhat the role of temperature at T_g [27,24]. The lower density at higher temperatures is also expected to enhance that role since H bonding is an orientation-specific interaction [28]. Our findings cannot be ascribed to the presence of side groups in PVAc. In fact, PALS measurements [53] in the main-chain 1,4 polybutadiene (PB) ($T_\beta = 210$ K [6]) evidenced only a very weak bend of τ_{o-PS} at 206 K.

In summary, we showed first that ESR is able to detect the splitting of the α and β relaxations in two model glass formers without resort to extrapolation or fitting procedures.

Having located the crossover region by ESR, we analyzed the PALS data in this region. Both ESR and PALS investigate the same length and time scales. We conclude that the crossover region is affected by the density in OTP but not in PVAc on the length scale of a few Å and the time scale of a few ns

S. Capaccioli, R. Casalini, G. Consolati, K.L. Ngai, and R. Richert are warmly thanked for useful discussions.

- [1] G. Williams, *Trans. Faraday Soc.* **60**, 1548 (1964); *Trans. Faraday Soc.* **61**, 1564 (1965).
- [2] P. B. Macedo and T. A. Litovitz, *J. Chem. Phys.* **42**, 245 (1965).
- [3] M. Goldstein, *J. Chem. Phys.* **51**, 3728 (1969).
- [4] G. P. Johari and M. Goldstein, *J. Chem. Phys.* **53**, 2372 (1970).
- [5] E. Rössler, *Phys. Rev. Lett.* **65**, 1595 (1990).
- [6] A. Arbe, D. Richter, J. Colmenero, and B. Farago, *Phys. Rev. E* **54**, 3853 (1996).
- [7] D. Gomez, A. Alegria, A. Arbe, and J. Colmenero, *Macromolecules* **34**, 503 (2001).
- [8] F. H. Stillinger, *Science* **267**, 1935 (1995).
- [9] F. Stickel, E. W. Fischer, and R. Richert, *J. Chem. Phys.* **102**, 6251 (1995); **104**, 2043 (1996).
- [10] K. L. Ngai, J. Magill, and D. J. Plazek, *J. Chem. Phys.* **112**, 1887 (2000).
- [11] K. L. Ngai, L. Bao, A. F. Yee, and C. L. Soles, *Phys. Rev. Lett.* **87**, 215901 (2001).
- [12] F. Fujara, B. Geil, H. Sillescu, and G. Fleischer, *Z. Phys. B: Condens. Matter* **88**, 195 (1992).
- [13] G. Heuberger and H. Sillescu, *J. Phys. Chem.* **100**, 15255 (1996).
- [14] A. Voronel *et al.*, *Phys. Rev. Lett.* **80**, 2630 (1998).
- [15] L. Andreozzi, F. Cianflone, C. Donati, and D. Leporini, *J. Phys.: Condens. Matter* **8**, 3795 (1996).
- [16] L. Andreozzi, A. DiSchino, M. Giordano, and D. Leporini, *J. Phys.: Condens. Matter* **8**, 9605 (1996).
- [17] L. Andreozzi, A. DiSchino, M. Giordano, and D. Leporini, *Europhys. Lett.* **38**, 669 (1997).
- [18] C. A. Angell, *Science* **267**, 1924 (1995).
- [19] K. U. Schug, H. E. King, and R. Böhmer, *J. Chem. Phys.* **109**, 1472 (1998).
- [20] M. Paluch, A. Patkowski, and E. Fischer, *Phys. Rev. Lett.* **85**, 2140 (2000).
- [21] H. Leyser, A. Schulte, W. Doster, and W. Petry, *Phys. Rev. E* **51**, 5899 (1995).
- [22] R. Casalini, S. Capaccioli, M. Lucchesi, P. A. Rolla, and S. Corezzi, *Phys. Rev. E* **63**, 031207 (2001).
- [23] R. Casalini, S. Capaccioli, M. Lucchesi, P. A. Rolla, M. Paluch, S. Corezzi, and D. Fioretto, *Phys. Rev. E* **64**, 041504 (2001).
- [24] M. L. Ferrer, C. Lavrence, B. G. Demirjian, D. Kivelson, C. Alba-Simonesco, and G. Tarjus, *J. Chem. Phys.* **109**, 8010

- (1998).
- [25] R. Casalini and C. M. Roland, *J. Chem. Phys.* **119**, 11 951 (2003).
- [26] M. Paluch *et al.*, *Phys. Rev. E* **68**, 031802 (2003).
- [27] C. M. Roland and R. Casalini, *Macromolecules* **36**, 1361 (2003).
- [28] M. Naoki, H. Endou, and K. Matsumoto, *J. Phys. Chem.* **91**, 4169 (1987).
- [29] M. Paluch *et al.*, *J. Chem. Phys.* **118**, 4578 (2003).
- [30] M. Paluch, R. Casalini, and C. M. Roland, *Phys. Rev. B* **66**, 092202 (2002).
- [31] K. Mpoukouvalas and G. Floudas, *Phys. Rev. E* **68**, 031801 (2003).
- [32] C. Dreyfus, A. Aouadi, J. Gapinski, M. Matos-Lopes, W. Steffen, A. Patkowski, and R. M. Pick, *Phys. Rev. E* **68**, 011204 (2003).
- [33] C. Alba-Simonesco, D. Kivelson, and G. Tarjus, *J. Chem. Phys.* **116**, 5033 (2002).
- [34] A. Barbieri, E. Campani, S. Capaccioli, and D. Leporini, *J. Chem. Phys.* **120**, 437 (2004).
- [35] C. Hansen, F. Stickel, T. Berger, R. Richert, and E. W. Fischer, *J. Chem. Phys.* **107**, 1086 (1997).
- [36] *Biological Magnetic Resonance*, edited by L. J. Berliner and J. Reuben (Plenum, New York, 1989), Vol. 8.
- [37] M. Faetti, M. Giordano, D. Leporini, and L. Pardi, *Macromolecules* **32**, 1876 (1999).
- [38] *Electron Spin Relaxation in Liquids*, edited by L. T. Muus and P. W. Atkins (Plenum, New York, 1972).
- [39] J. P. Hansen and I. R. McDonald, *Theory of Simple Liquids* 2nd edition (Academic Press, New York, 1986).
- [40] Y. C. Jean and H. Shi, *J. Non-Cryst. Solids* **172-174**, 806 (1994).
- [41] G. Consolati, *J. Chem. Phys.* **117**, 7279 (2002).
- [42] C. L. Wang, T. Hirade, F. H. J. Maurer, M. Eldrup, and N. J. Pedersen, *J. Chem. Phys.* **108**, 4654 (1998).
- [43] R. Richert and C. A. Angell, *J. Chem. Phys.* **108**, 9016 (1998).
- [44] H. Wagner and R. Richert, *J. Phys. Chem. B* **103**, 4071 (1999).
- [45] C. A. Angell, K. L. Ngai, G. B. McKenna, P. F. McMillan, and S. W. Martin, *J. Appl. Phys.* **88**, 3113 (2000).
- [46] W. Steffen, A. Patkowski, H. Gläser, G. Meier, and E. W. Fischer, *Phys. Rev. E* **49**, 2992 (1994).
- [47] W. Steffen, B. Zimmer, A. Patkowski, G. Meier, and E. W. Fischer, *J. Non-Cryst. Solids* **172-174**, 37 (1994).
- [48] M. Cicerone, F. R. Blackburn, and M. D. Ediger, *J. Chem. Phys.* **102**, 471 (1995).
- [49] N. G. McCrum, B. E. Read, and G. Williams, *Anelastic and Dielectric Effects in Polymeric Solids* (Wiley, New York, 1967).
- [50] Sz. Vass, A. Patkowski, E. W. Fischer, K. Süvegh, and A. Vertes, *Europhys. Lett.* **46**, 815 (1999).
- [51] M. Beiner, J. Korus, H. Lockwenz, K. Schroter, and E. Donth, *Macromolecules* **29**, 5183 (1996).
- [52] G. Williams, *Adv. Polym. Sci.* **33**, 60 (1979).
- [53] J. Bartos *et al.*, *J. Non-Cryst. Solids* **307-310**, 417 (2002).